JOURNAL OF CATALYSIS 38, 153–165 (1975)

The Interaction of Hydrogen and Carbon Monoxide on Polycrystalline Nickel Films at Temperatures up to 353 K

G. WEDLER, H. PAPP AND G. SCHROLL

Institut für Physikalische Chemie II, Universtität Erlangen-Nürnberg, 8520 Erlangen, Germany

Received July 1, 1974

The interaction of H_2 and CO on nickel films at 77, 273 and 353 K was investigated by measurements of thermal desorption, electrical resistance and changes in work function. For this purpose the adsorption of H_2 on nickel films partially covered with CO, the adsorption of CO on nickel films partially covered with H_2, and the alternating adsorption of H_2 and CO were studied.

Although reaction products of H_2 and CO could not be found under the experimental conditions chosen, clear evidence for their interaction could be seen. This interaction could be recognized by an increase in the heat of adsorption of H_2 due to the presence of CO, an increase in the amount of CO adsorbed on nickel films due to the presence of H_2, and the CO-induced transformation of H_2, adsorbed in the β_2 phase, into another phase.

I. INTRODUCTION

For the reaction of H_2 and CO on metal catalysts, the formation of an adduct

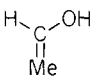

has been assumed by different authors (*1–4*) as a preliminary step which is independent of the reaction products. Several attempts have been made to obtain experimental evidence for the existence of such an intermediate product. Kölbel and his co-workers obtained the first indications of an adsorption complex from calorimetric (*5*), kinetic (*6*) and desorption measurements (*7*) on supported iron catalysts. Infrared absorption bands of a C–OH bond were found on nickel catalysts above 453 K (*8*).

The discussion of the results, however, was especially difficult when technical catalysts were used and too many parameters may influence the results. Therefore it is preferable to study the interaction of CO and H_2 on pure metals by means of evaporated films or single crystals, which show better reproducibility. On those materials ir spectra (*9*), heats of adsorption (*10–12*), adsorption isotherms (*13*), flash desorption spectra (*14–16*), changes in work function (*15,17*), changes in electrical resistance (*12,18*), and the sticking probability (*19*) were measured.

The separate adsorption of H_2 and CO on nickel films has been investigated by measuring the change in electrical resistance (*20–25*), the work function (*25,26*), the differential heat of adsorption (*20,25,27–30*), thermal desorption spectra (*31,32*), and mass spectra (*31–33*). Therefore it seemed to be sensible to look for the mutual interaction of H_2 and CO on nickel films by using the same techniques. Reaction products are not very likely at the temperature and pressure conditions chosen (*8*). The effects observed probably derive from primary interactions between adsorbed H_2 and adsorbed CO.

II. EXPERIMENTAL METHODS

The experimental methods used are fully described elsewhere (*31,33–35*).

The glass UHV apparatus gave vacua of 2×10^{-10} Torr. The nickel films were condensed at this pressure on cooled (77 K) glass bulbs at a rate of about 10 Å/min until a thickness of about 100 Å was obtained. Sintering for 1 hr at 333 or 373 K was used to produce films in a more ordered state. They consist then mainly of crystallites which show the (111) and, to a lower extent, the (100) planes on their surfaces (*36,37*).

CO and H_2 were adsorbed on the films in various sequences. CO was added from ampoules, H_2 from ampoules or from a UHV gas pipette. CO was produced by thermal decomposition of calcium oxalate; H_2 was introduced by diffusion through a palladium tube. In both cases the mass spectrometric analysis showed a purity of more than 99%. The slight contamination of CO was mainly due to H_2 and He; H_2 was contaminated by rare gases.

The measurements of the electrical resistance were made by means of Wheatstone bridge (*35*), the change in work function was investigated by a retarding-field diode (*38*), the differential heat of adsorption was determined by calorimetric measurements (*20,27,34*), and the thermal desorption was measured in the same way as in the system Ni/H_2 (*31*). The white-hot cathode of the diode can cause atomization or ionization of the gases. To avoid these effects the cathode was only used when the pressure in the gas phase had fallen below 10^{-7} Torr after each gas addition. However, the hot cathode can be used to produce atomic hydrogen for adsorption.

Because of the mass spectrometric analysis it is often better to use deuterium as an adsorbate instead of hydrogen.

III. THE SYSTEMS Ni/H_2 AND Ni/CO

The systems Ni/H_2 and Ni/CO have already been described in detail. A short summary of the results is given here. It is advisable to observe the results of the systems consisting only of one adsorbent and one adsorbate as a function of the fraction θ of the monolayer coverage (*25*). The monolayer coverage is defined by the termination of chemisorption, i.e., for instance, when the heat of adsorption drops to very low values. This coverage is a function of the adsorbate and of the roughness of the films. The monolayer H_2 coverage is 15×10^{14} molecules H_2 cm^{-2} on nickel films which were sintered at 333 K, and 10×10^{14} molecules H_2 cm^{-2} on nickel films which were sintered at 373 K. The value for CO is 17.5×10^{14} molecules CO cm^{-2} at both sinter temperatures.

The results obtained with the system Ni/H_2 (*20,21,26,28,29,31,39*) are listed below.

1. At coverages below half a monolayer H_2 is atomically adsorbed causing an increase in the electrical resistance (*20*) and in the work function (*26*) independent of the temperature between 77 and 273 K. The heat of adsorption decreases from 18 to 16 kcal/mole (*20,29*). H_2 is adsorbed in a uniform state (β_2) which can be recognized by a pressure maximum at 360 K in the thermal desorption spectrum (*31*).

2. A further atomic adsorption takes place as the coverage is increased to a monolayer. This adsorption leads to a decrease in the electrical resistance (*20,21*) and a slight increase in the work function (*26*). The differential heat of adsorption shows a maximum and then drops to low values at 273 K (*20,29*). At 77 K the heat of adsorption decreases continuously (*20,29*). A further peak (β_1) can be seen in the thermal desorption spectrum at 320 K (*31*). When the adsorbate has sufficient mobility [above 181 K (*39*)] both states, β_1 and β_2, are interconverted.

3. A coverage of more than one monolayer cannot be achieved above 77 K under the applied pressures ($p \leq 10^{-2}$ Torr). At 77 K in addition to the effects listed in paragraph 2, a molecular adsorp-

TABLE 1
SUMMARY OF RESULTS FOR THE SYSTEMS Ni/H_2 AND Ni/CO

Coverage θ	Effect	Ni/H_2	Refs.	Ni/CO	Refs.
$0 < \theta \leq 0.5$	ΔR	>0	(20, 21)	>0	(21, 23, 24, 25)
	$\Delta\phi/V$	$0 \rightarrow 0.23$	(26, 43)	$0 \rightarrow 0.9$	(25)
	q/kcal mole^{-1}	$18 \rightarrow 16$	(20, 28, 29)	$30 \rightarrow 25$	(30)
	Desorption peaks	360 K (β_2)	(31)	460 K (β_2)	(32)
$0.5 \leq \theta \leq 1.0$	ΔR	<0	(20, 21)	<0	(25)
	$\Delta\phi/V$	$0 \rightarrow 0.25$	(26, 43)	$0 \rightarrow 1.4$	(25)
	q/kcal mole^{-1}	$16 \rightarrow <5$	(20, 28, 29)	$25 \rightarrow <5$	(30)
	Desorption peaks	360 K (β_2), 300 K (β_1)	(31)	460 K (β_2), 330 K (β_1)	(32)
$\theta > 1.0$	ΔR	>0	(20)	>0	(25)
	$\Delta\phi/V$	<0	(40)	0	(25)
	q/kcal mole^{-1}	<1	(41)	—	
	Desorption peaks	360 K (β_2), 300 K (β_1), 90 K (γ)	(31)	460 K (β_2), 310 K (β_1), 170 K (γ)	(32)

tion of H_2 takes place, which causes an increase in the electrical resistance (*20*) and a decrease in the work function (*40*). The heat of adsorption is smaller than 1 kcal/mole (*41*); there is a further pressure peak (γ) at 90 K in the thermal desorption spectrum (*31*).

Qualitatively the same effects are found for the system Ni/CO (*21,25,33*); quantitatively there is a tighter bond to the adsorbent, as can be seen in Table 1.

The system Ni/D_2 differs from the system Ni/H_2 only in the heat of adsorption which is 1 kcal/mole higher (*28*). This causes an insignificant shift of the desorption peaks to higher temperatures (*42,43*). Therefore, in the following discussion both H_2 and D_2 will be referred to as hydrogen.

IV. COADSORPTION OF H_2 AND CO ON NICKEL FILMS

A. Adsorption of H_2 on Nickel Films After Preadsorption of CO

1. Adsorption Temperature 77 K

a. Adsorption of molecular H_2. Figure 1a shows the change in resistivity $\Delta\rho$ mul-

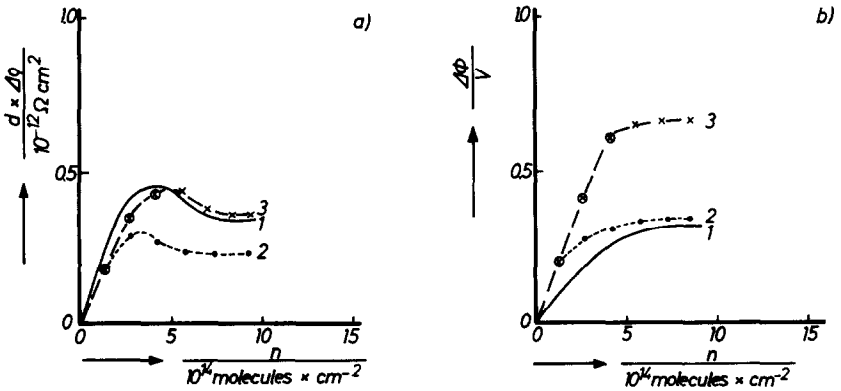

FIG. 1. Influence of H_2 adsorption on the resistivity (a) and the work function (b) of nickel films at 77 K. Precoverage with CO: (1) $\theta_{CO} = 0$; (2) $\theta_{CO} = 0.15$; (3) $\theta_{CO} = 0.5$. The encircled points are for CO adsorption.

tiplied by the film thickness d (*22,44*) as a function of coverage. The solid line 1 refers to H_2 adsorption on a clean nickel film. After a complete H_2 desorption (cf. line 1 in Fig. 2) 1.4×10^{14} molecules CO cm^{-2}, corresponding to 15% of a monolayer based on H_2, were adsorbed on the same film. The subsequent H_2 adsorption caused a change in the electrical resistance (cf. line 2 in Fig. 1a) which is qualitatively the same as for a pure H_2 adsorption in this region of coverage (cf. line 1 in Fig. 1a). The quantity of CO plus H_2 which could be adsorbed is in accordance with the monolayer quantity for a pure H_2 adsorption. The amount of H_2 which was added in the second cycle could again be desorbed completely, whereas the CO remained on the film at temperatures below 400 K. In a third cycle the CO precoverage was increased to 4.1×10^{15} molecules CO cm^{-2}, corresponding to about half a monolayer based on H_2. The following H_2 adsorption led to the same maximum coverage as in cycles 1 and 2. There again no influence of the precoverage was seen in the qualitative form of the resistance curve.

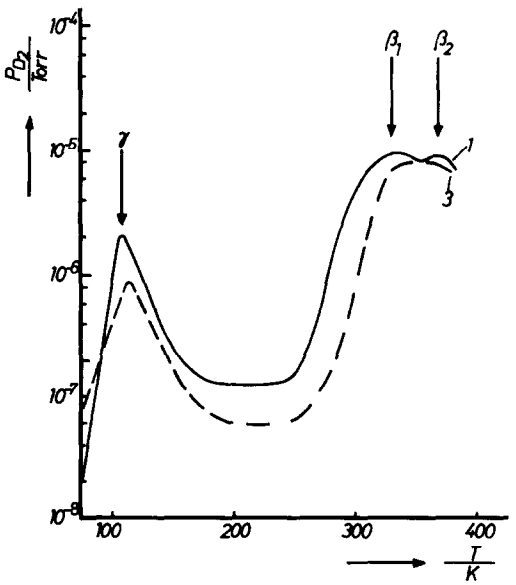

FIG. 2. Thermal desorption of H_2 from nickel films without CO precoverage (1) and with half monolayer CO precoverage (3).

When the CO coverage exceeded the monolayer H_2 coverage, no additional H_2 chemisorption could be seen. Horgan and King (*19*) obtained the same result.

Figure 1b shows the changes in work function which were observed in the three cycles described. It can be seen that the CO precoverage has only a weak influence on the change in the work function arising from the subsequent H_2 adsorption.

The change in resistivity as well as the change in work function indicate that the H_2 added in the third cycle of the adsorption should exist in a state which is similar to the β_1 state of pure H_2 adsorption. But the desorption spectra (cf. Fig. 2) show clearly that the adsorbed H_2 after CO precoverage (line 3 in Fig. 2) is bound tighter than H_2 in the β_1 state adsorbed on a clean nickel film (cf. line 1 in Fig. 2). This indicates an interaction between H_2 and CO.

b. Adsorption of atomic hydrogen. No chemisorption of H_2 molecules could be observed on a CO layer with a coverage greater than the H_2 monolayer. But a large amount of hydrogen atoms can be adsorbed on this CO layer. This adsorption causes the work function to decrease proportionally with the coverage, as reported by other authors (*17*). At the same time the electrical resistance increases. These facts are shown in Fig. 3.

The desorption peak (α) of H_2 added as atoms (cf. Fig. 4) clearly differs from the peaks β_1 and β_2, which are found after pure H_2 adsorption (*31*). This peak also differs from the peak of H_2 produced by molecular addition after CO precoverage (cf. Fig. 2). The desorption maximum (α in Fig. 4) is approximately at 300 K, which is clearly below other maxima. This desorption temperature is in accordance with the results of Siddiqi and Tompkins (*17*). They state that 50% of H_2 which was atomically added and adsorbed on a CO layer at 77 K desorb below 293 K and that the re-

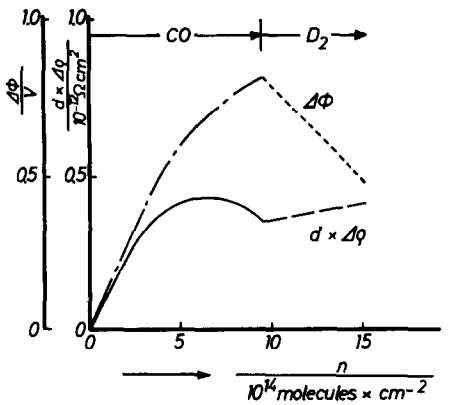

FIG. 3. Influence of the adsorption of atomic hydrogen on the resistivity ρ and the work function ϕ after a monolayer CO precoverage.

maining H_2 can be removed from the nickel film by pumping for 1 hr. These authors (*17*) assume that this H_2 exists in a positively polarized state within the chemisorbed CO monolayer.

2. *Adsorption Temperature 273 K*

The change in the electrical resistance at 273 K due to the chemisorption of H_2 on nickel films, which were partly covered with CO, has already been published (*12*). These results are in accordance with those at 77 K described in Sect. IV.A.1.a. and shown in Fig. 1a.

From the shift of the desorption peak of H_2 to higher temperatures—caused by the CO precoverage (cf. Fig. 2)—it was concluded that there would be a more tightly bound form of H_2 at 77 K due to the CO precoverage. At 273 K the heats of adsorption of H_2 on nickel films, partly covered with CO, show a clear increase compared with those of a pure H_2 adsorption. As shown in Fig. 5 the increase Δq is about 3–5 kcal/mole. It is especially striking that this difference remains constant over a wide range of coverage even at a low CO precoverage. This is an argument against the formation of a stoichiometric adsorption complex

as mentioned in the literature (*4–7*), because the amount of H_2 taken up with increased heat of adsorption is more than three times the preadsorbed amount of CO.

When a nickel film is covered with an amount of CO which exceeds the monolayer coverage based on H_2, a very slow

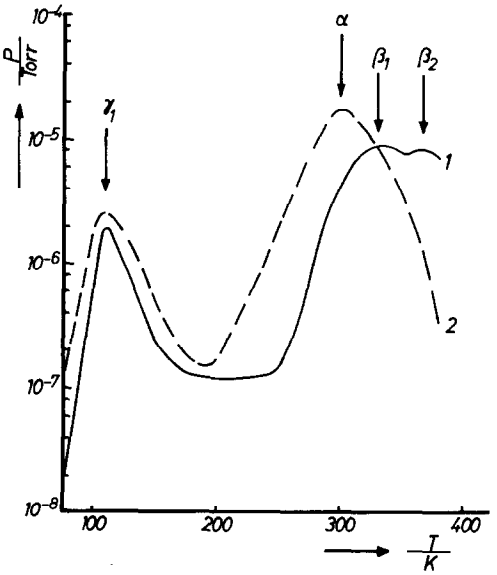

FIG. 4. Thermal desorption of H_2 from nickel films, which was added molecularly, without CO precoverage (1) and thermal desorption of H_2 from nickel films, which was added atomically, after a monolayer CO precoverage (2).

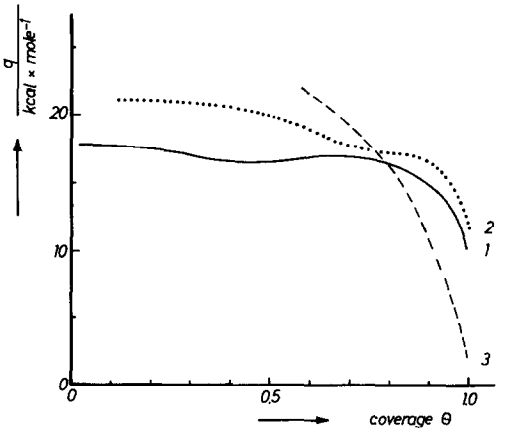

FIG. 5. Differential heat of adsorption q of H_2 on nickel films at 273 K. Procoverage with CO: (1) $\theta_{CO} = 0$; (2) $\theta_{CO} = 0.1$; (3) $\theta_{CO} = 0.6$.

H_2 adsorption can be seen at 273 K when H_2 molecules are added. This is in contrast to the case at 77 K and to the statements of Horgan and King (*19*). This adsorption, which only insignificantly increases the electrical resistance, is reversible, i.e., H_2 can be easily pumped off. From the change in the temperature of the calorimeter it can be concluded that the H_2 adsorption is endothermic. Due to the very slow rate of adsorption a quantitative analysis of the calorimetric data was impossible. By means of work function measurements one might be able to decide whether this state of adsorption is identical to the α state at 77 K. As a result of the high gas pressure no measurements were possible with the diode.

No displacement of CO by H_2 was observed at 77 and 273 K.

B. Adsorption of CO on Nickel Films After Precoverage with H_2

1. Adsorption Temperature 77 K

Figure 6 shows the change in resistivity due to the adsorption of H_2 followed by adsorption of CO. H_2 was adsorbed up to a monolayer; this adsorption was accompanied by the well-known change in resistivity. Then CO was added until a perceptible CO partial pressure could be noticed. The change in resisitivity due to this adsorption was quite different from that on a clean film. At first (region I in Fig. 6) the slope of the resistivity curve is gentler than on clean films. At $n = 6 \times 10^{14}$ molecules CO cm^{-2} the curve reaches a point of inflection and at 22×10^{14} molecules CO cm^{-2}, when CO showed a noticeable pressure, the change in resistivity reaches a saturation value. This saturation value is about the same as on clean nickel films. The explanation of this change in resistivity is given at the end of paragraph IV.B.2 in connection with simular results at 273 K.

Throughout the whole adsorption of CO at 77 K no H_2 was displaced. The amount of adsorbed CO was about the same as on a clean Ni film at 77 K. Therefore the total amount of adsorbed gas equaled one monolayer of H_2 plus one monolayer of CO.

In a fresh experiment H_2 was first adsorbed to more than a monolayer giving some physically adsorbed H_2 in the γ state in addition to the β_1 and β_2 states (cf. Table 1). During the following CO adsorp-

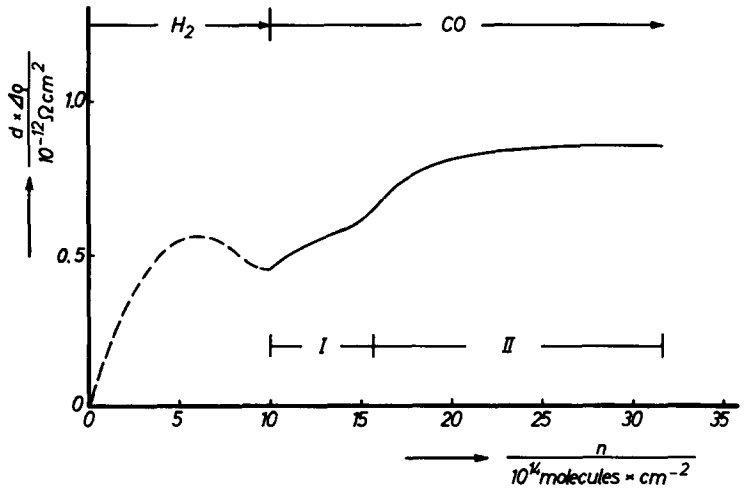

FIG. 6. The change in resistivity $\Delta\rho$ due to H_2 adsorption (up to 10×10^{14} molecules H_2 cm^{-2}) and subsequent CO adsorption. Adsorption temperature 77 K.

tion this physically adsorbed H_2 was displaced immediately into the gas phase.

The observations at 77 K mentioned above are in good agreement with the results obtained by Horgan and King (*19*).

2. Adsorption Temperature 273 K

At 273 K matters become more complicated when a nickel film is first covered with H_2, and then followed by CO adsorption.

In Fig. 7 the total pressure in the gas phase (–··), the partial pressure of H_2 (broken line) and the partial pressure of CO (solid line) are plotted versus coverage. During H_2 adsorption up to $\theta_{H_2} \approx 0.5$ the gas phase pressure was only due to helium (dotted line) which had diffused into the H_2 ampoules. It was pumped off. The following CO adsorption did not significantly increase the pressure until the total coverage had reached the monolayer coverage based on H_2, at $n = 13 \times 10^{14}$ molecules cm^{-2}. The partial pressure analysis indicated mainly H_2, apart from minor contaminants consisting of methane and helium, which had been in the CO ampoules (*33*). This H_2 must have been displaced from the film by CO. As soon as 17×10^{14} molecules CO cm^{-2} had been adsorbed (corresponding to a monolayer of CO on a clean nickel film), the CO partial pressure in the gas phase rose. Further CO added was hardly adsorbed at all and therefore remained mainly in the gas phase. At the same time the H_2 partial pressure started decreasing again. This effect is identical with the slow H_2 adsorption on a CO monolayer already described in Sect. IV.A.2. No reaction products were observed in the gas phase.

The differential heat of reaction q_{CO}, the change in work function $\Delta\phi$, and the change in resistivity $\Delta\rho$ multiplied by the film thickness d are plotted in Fig. 8 versus the coverage of H_2 and CO. Prior to these measurements the film had been sintered at 373 K and therefore showed a slightly lower capacity for adsorbing gas then the film in Fig. 7. The H_2 coverage was $\theta_{H_2} \approx 0.5$. The arrows *a* and *b* mark the appearance of H_2 and CO, respectively, in the gas phase (cf. Fig. 7). The effects observed as a result of H_2 adsorption are the usual ones on clean nickel films (cf. Table 1). During the following CO adsorption the change in work function could be measured only until a perceptible equilibrium pressure occurred. The dipole moment,

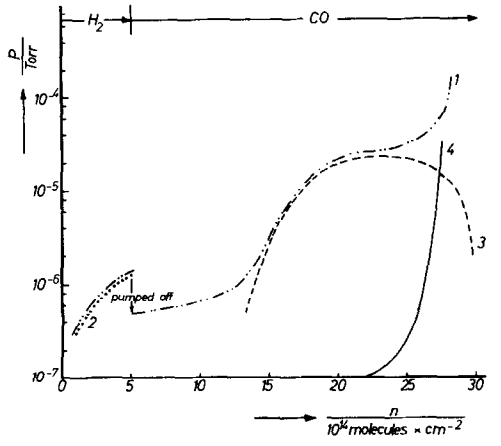

FIG. 7. Analysis of the gas phase during CO adsorption on a nickel film precovered with 5×10^{14} molecules H_2 cm^{-2} at 273 K. (1) Total pressure; (2) He partial pressure; (3) H_2 partial pressure; (4) CO partial pressure.

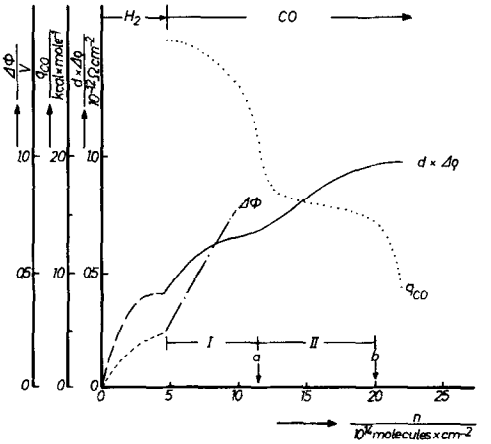

FIG. 8. The change in work function ϕ, resistivity ρ, and net heat of reaction q due to CO adsorption on a nickel film (thickness d) at 273 K after a H_2 precoverage until $n = 5 \times 10^{14}$ molecules H_2 cm^{-2}.

which can be calculated from the slope, is only 10% lower than for CO adsorption on a clean nickel film. q_{CO} is the net heat of reaction for all effects accompanying the chemisorption of 1 mole of CO. The value of q_{CO} initially measured is about the same as for the heat of adsorption of CO on a clean nickel film at low coverage. Then q_{CO} drops to about 18 kcal/mole. This value has just been reached, when the H_2 partial pressure starts rising noticeably (cf. arrow *a* in Fig. 8). Between the arrows *a* and *b* the H_2 partial pressure increases proportionally to the amount of CO added. The curve of the heat of reaction q_{CO} in this region shows a plateau with an average value of 16 kcal/mole. When the CO partial pressure starts to rise (cf. arrow *b* in Fig. 8) q_{CO} has the value of 15 kcal/mole. Then q_{CO} slumps to low values.

The two sections, CO adsorption without H_2 displacement (until arrow *a*), and CO adsorption with H_2 displacement (*a* to *b*) stand out clearly in the resisitivity curve ($d \times \Delta\rho$) in a way which is very similar to that at 77 K.

Before the curves can be discussed in detail the quantity of H_2 displaced by CO should be expressed as a function of the CO coverage. Figure 9 shows this relationship for two different experiments. Curve 1 was obtained when no gas was pumped off and the mass spectrometric analysis of the gas phase was always made at the same time (10 min after each CO addition). This curve is in accordance with the broken line in Fig. 7. If the displaced H_2 was pumped off immediately after each CO adsorption, in order to prevent the readsorption of displaced H_2, and the pumped-off gas is collected in a known volume, one obtains curve 2 in Fig. 9 for the amount of H_2 displaced. It is obvious that at the first appearance of a perceptible CO pressure (curve 3 in Fig. 9) the whole of the H_2 originally adsorbed had been displaced from the film.

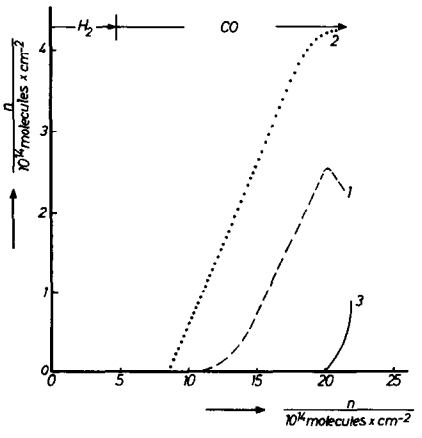

FIG. 9. Displacement of preadsorbed H_2 (molecules cm^{-2}) due to a subsequent CO adsorption at 273 K. (1) Displaced amount of H_2 without pumping; (2) displaced amount of H_2 when pumped off; (3) amount of CO not adsorbed.

In order to interpret the effects plotted in Figs. 7 to 9, the following mechanism is taken as a basis for the interaction of the two gases:

1. H_2 is only added up to half a monolayer coverage. Therefore it is adsorbed in the state β_2 causing an increase in the electrical resistance (cf. Sect. III).

2. As long as the overall coverage does not exceed the monolayer coverage based on H_2, the adsorbed CO increases the electrical resistance without displacing H_2 into the gas phase. H_2 originally adsorbed in state β_2 changes into another state which leads to a decrease in the electrical resistance. This state might be similar to the β_1 state of H_2 adsorbed on a clean nickel film (cf. Table 1).

3. When the total coverage exceeds the monolayer coverage based on H_2, H_2 is displaced from the film into the gas phase by CO.

4. H_2 is slowly readsorbed on the CO layer from the gas phase.

In order to interpret the curve of resistivity in Fig. 8 it is advisable to compare it with the change in resistivity which is due to CO adsorption on a clean nickel film. In Fig. 10 these two curves are plotted versus the coverage and, as shown, the same final value of $d \times \Delta\rho$ has been achieved in both

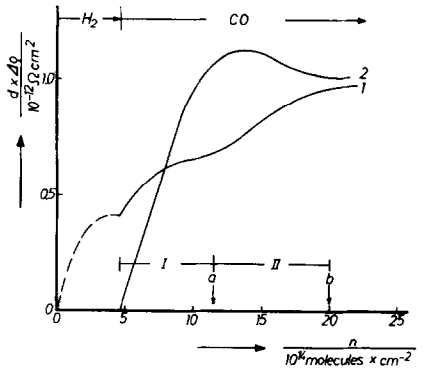

FIG. 10. The change in resistivity $\Delta\rho$ multiplied by the film thickness d due to H_2 adsorption ($\theta = 0.5$), followed by CO adsorption (1) and due to pure CO adsorption (2); $T = 273$ K.

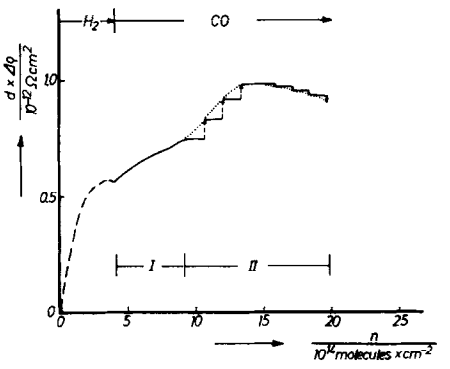

FIG. 11. The change in resistivity $\Delta\rho$ multiplied by the film thickness d due to H_2 adsorption ($\theta = 0.5$) followed by CO adsorption. The arrows show the change in resistivity caused by pumping off the displaced H_2; $T = 273$ K.

cases; i.e., preadsorption of H_2 followed by CO adsorption which is connected with a displacement of H_2 (line 1) and adsorption of CO on a clean nickel film (line 2).

In region I, i.e., before H_2 is displaced into the gas phase, the change in resistivity due to CO adsorption is less than it would be during a CO adsorption on a clean nickel film.

According to the hypothesis assumed the change in resistivity in this section should be composed of two effects, namely the increase in resistivity due to CO adsorption and the decrease in resistivity caused by the transformation of H_2 from the state β_2 into a new state. The expected minor increase in resistivity was in fact observed.

In region II H_2 is displaced and the change in resistivity should again be composed of two effects, namely a slight change in resistivity due to the CO adsorption and an increase in resistivity due to the H_2 displacement. The latter effect can be proved experimentally when, in region II, H_2 is not only displaced (line 1 in Fig. 9) but is also removed by pumping (curve 2 in Fig. 9). The result is shown in Fig. 11: although the CO adsorption only changes the resistance slightly the resistance is then increased by pumping off H_2. The slight reversal of this effect above $n = 15 \times 10^{14}$ molecules cm^{-2} remains unexplained.

The plateau in the q_{CO} curve plotted in Fig. 8 is situated in region II, where H_2 is displaced from the film by CO. The slope of line 1 in Fig. 9 indicates that about two CO molecules are necessary to displace one H_2 molecule under the experimental conditions chosen.

In the first approximation the whole process of displacement can be divided into three steps:

a. adsorption of CO

$$2Ni + 2CO \rightarrow 2Ni\text{-}CO$$

$$\Delta H = 2\left(-25 \frac{\text{kcal}}{\text{mole CO}}\right);$$

b. breaking of the chemisorption bond Ni-H

$$2Ni\text{-}H \rightarrow 2Ni + 2H^*$$

$$\Delta H = 2\left(61 \frac{\text{kcal}}{\text{mole Ni H}}\right);$$

c. recombination of the hydrogen atoms

$$2H^* \rightarrow H_2 \qquad \Delta H = -104 \frac{\text{kcal}}{\text{mole } H_2}.$$

Therefore the overall reaction,

$$2Ni\text{-}H + 2CO \rightarrow 2Ni\text{-}CO + H_2$$

$$\Delta H = 2\left(-16 \frac{\text{kcal}}{\text{mole CO}}\right),$$

should show a heat of reaction $q_{CO} = (-16$ kcal/mole CO). This is in good agreement with the experimental results (cf. Fig. 8). H* stands for a hydrogen atom which is no longer chemisorbed.

After the explanation of the results at 273 K it is now possible to return to the observations at 77 K.

Again the change in resistivity due to H_2 adsorption and to the subsequent CO adsorption at 77 K (cf. Fig. 6 of Sect. IV.B.1.) can be explained by the transformation of the chemisorbed H_2. In region I of Fig. 6 β_2-H_2, which originally increases the resistivity, is transformed by CO into another state, thus producing a smaller overall increase in resistivity than that due to the CO adsorption. In region II of Fig. 6 β_1-H_2, which originally decreases the resistivity, is transformed by the adsorption of CO into another state. This process is reflected by a higher increase in resistivity at the beginning of region II in Fig. 6.

In contrast to 273 K there is no displacement of chemisorbed H_2 into the gas phase at 77 K. At 273 K hydrogen is mobile on a nickel surface, whereas at 77 K it has no mobility (*39*). Probably this immobility prevents step c of the mechanism of the hydrogen displacement assumed above, i.e., the recombination of the hydrogen atoms. These hydrogen atoms remain therefore on the nickel surface.

3. *Adsorption Temperature 353 K*

At 353 K it was not possible to achieve the necessary constant temperature for calorimetric measurements. Furthermore the equilibrium pressure was too high for measurements with the diode. Therefore Fig. 12 shows only the change in resistivity. In Fig. 13 the amount of H_2 displaced from the film and the amount of CO remaining in the gas phase are plotted (same scales as Fig. 9) versus the total coverage. The H_2 coverage at 353 K reaches only half a monolayer at an equilibrium pressure of 10^{-6} Torr. H_2 is displaced immediately

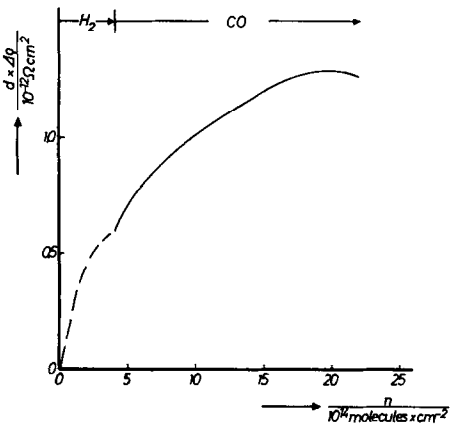

FIG. 12. The change in resistivity $\Delta\rho$ multiplied by the film thickness d due to H_2 adsorption ($\theta = 0.5$) followed by CO adsorption; $T = 353$ K.

from the film by the following CO adsorption (cf. Fig. 13). Therefore there is no region I in Fig. 13 such as that in Figs. 8, 10 and 11 for adsorption at 273 K. This fact can also clearly be seen in the change in resistivity due to CO adsorption (cf. Fig. 12).

Although H_2 was very easily displaced from the film at 353 K a readsorption of this gas on the CO layer could be observed as at 273 K.

It is striking that the presence of H_2 doubles the capacity of nickel films for CO uptake at 353 K in comparison with the

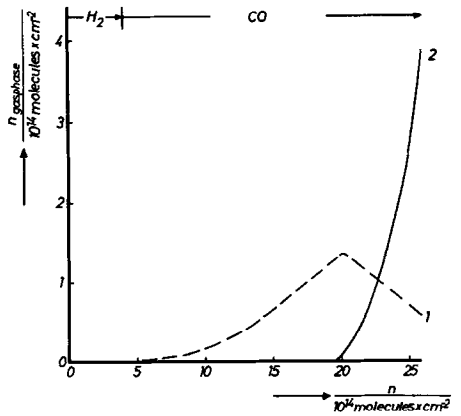

FIG. 13. Displacement of preadsorbed H_2 due to a following CO adsorption at 353 K. (1) Displaced amount of H_2 without pumping; (2) the amount of CO in the gas phase.

uptake for CO on clean nickel films. A similar observation was made by Horgan and King at 373 K (*19*).

C. Alternating H_2 and CO Adsorption at 273 K

In Figs. 14 and 15 the results of an experiment are shown in which a nickel film was alternately covered with small quantities of H_2 and CO. The arrows *a* and *b*, respectively, indicate at which coverage the H_2 and CO pressure rose.

The two figures sum up the effects which were caused by H_2 adsorption after a CO precoverage (cf. Sect. IV.A) as well as the effects which were caused by CO adsorption after a H_2 precoverage (cf. Sect. IV.B). These are as follows.

The resistivity curves of region I show no mutual interaction of the gases (cf. Fig. 1a). The experiment confirms that at low coverages CO and H_2 adsorption produce the same slope of the resistivity curve.

The increase in the heat of adsorption of H_2 compared with the value achieved on a clean nickel film indicates that there must be an interaction between the two gases (cf. Fig. 5). Whether the heat of adsorption of CO is influenced by H_2 cannot be proved definitely.

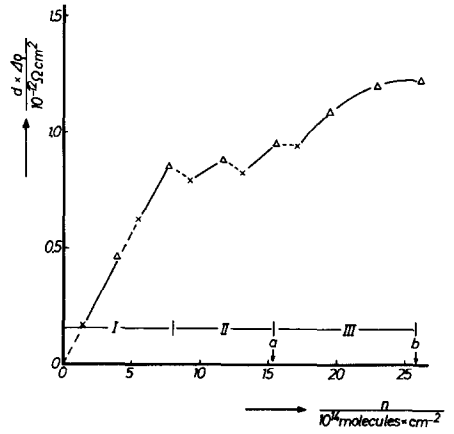

FIG. 14. The change in resistivity $\Delta\rho$ multiplied by the film thickness *d* caused by an alternating H_2 (×) and CO (△) adsorption on a nickel film at 273 K. Arrow *a* indicates the coverage at which H_2 appears in the gas phase.

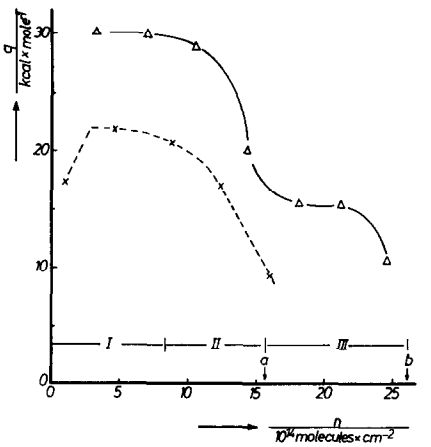

FIG. 15. The differential heat of adsorption during an alternating H_2 (×) and CO (△) adsorption on a nickel film at 273 K. Arrow *a* indicates the coverage at which H_2 appears in the gas phase. Arrow *b* indicates the coverage at which CO appears in the gas phase.

In region II the H_2 adsorption leads to a decrease in resistivity, as when H_2 is adsorbed on a clean nickel film beyond half monolayer coverage (cf. Fig. 1a). In the same region the increase in resistivity due to CO adsorption is considerably smaller than on a clean nickel film. This is an indication that H_2 passes from the β_2 state into another state (cf. Sect. IV.B.2). The heat of adsorption q_{H_2} of H_2 drops to low values, and the net heat of reaction q_{CO} of CO falls to the plateau at 16 kcal/mole (cf. Fig. 8).

Finally, in region III, H_2 is displaced by CO into the gas phase. The net heat of reaction q_{CO} during this process is about 16 kcal/mole, as it was in Sect. IV.B.2. At the end of region III q_{CO} drops to low values and little CO is adsorbed. The change in resistivity in this region is the same as is known from Sect. IV.B.2.

SUMMARY

No reaction products could be found in the gas phase as a result of the simultaneous adsorption of CO and H_2 on nickel films within the investigated range of temperature of 77 to 353 K. Moreover, there

were no signs of the formation of a reaction product on the surface. This is in agreement with the results of Blyholder and Neff (*8*), who did not find any reaction products below 453 K when they investigated the interaction of CO and H_2 on nickel/silica catalysts by means of ir measurements.

Despite this, a series of results indicate a considerable interaction between the two gases:

1. The heat of adsorption of H_2 is increased by the presence of preadsorbed CO.

2. H_2 is readsorbed on a CO layer at 273 K and higher temperatures.

3. The capacity of the films for CO uptake is considerably increased at 353 K by the presence of H_2. Horgan and King (*19*) reported such an effect at 300 K. At 273 K, however, this effect cannot be seen.

The other effects reported can be traced back to the fact that CO is more strongly adsorbed on nickel than H_2:

1. CO can change H_2 from the β_2 state into another adsorbed state, when the total coverage exceeds half monolayer coverage based on H_2.

2. When the total coverage exceeds the monolayer coverage based on H_2, H_2 is displaced into the gas phase by CO. Lapujoulade (*16*) obtained similar results by means of kinetic experiments.

ACKNOWLEDGMENTS

The authors are indebted to the Deutsche Forschungsgemeinschaft and the Verband der chemischen Industrie for the financial support of this work.

REFERENCES

1. Storch, H. H., *in* "Advances in Catalysis" (W. G. Frankenburg, V. I. Komarewsky and E. K. Rideal, Eds.), Vol. 1, p. 115. Academic Press, New York, 1948.
2. Storch, H. H., Golumbic, N., and Anderson, R. B., "The Fischer-Tropsch and Related Syntheses." Wiley, New York, 1951.
3. Anderson, R. B., Hofer, L. J., and Storch, H. H., *Chem. Ing.-Techn.* **30,** 560 (1958).
4. Kölbel, H., "Chemische Technologie," Vol. 3, p. 439. Carl-Hauser-Verlag, München, 1959.
5. Kölbel, H., and Roberg, H., *Ber. Bunsenges. Phys. Chem.* **75,** 1100 (1971).
6. Kölbel, H., Engelhardt, F., Hammer, H., and Gaube, J., *Actes Congr. Int. Catal., 2nd, 1960,* 953 (1961).
7. Kölbel, H., Patzschke, G., and Hammer, H., *Z. Phys. Chem. (Frankfurt am Main)* **48,** 145 (1966).
8. Blyholder, G., and Neff, L. D., *J. Catal.* **2,** 138 (1963).
9. Harrod, J. F., Roberts, R. W., and Rissmann, E. F., *J. Phys. Chem.* **71,** 343 (1967).
10. Bagg, J., and Tompkins, F. C., *Trans. Faraday Soc.* **51,** 1071 (1955).
11. Klemperer, D. F., and Stone, F. S., *Proc. Roy. Soc., Ser. A* **243,** 375 (1957).
12. Wedler, G., and Bröcker, F. J., *Z. Phys. Chem. (Frankfurt am Main)* **75,** 299 (1971).
13. McKee, D. W., *J. Catal.* **8,** 240 (1967).
14. Baldwin, V. H., and Hudson, J. B., *J. Vac. Sci. Technol.* **8,** 49 (1971).
15. Yates, J. T., and Madey, T. E., *J. Chem. Phys.* **54,** 4969 (1971).
16. Lapujoulade, J., *J. Chim. Phys.* **68,** 73 (1971).
17. Siddiqi, M. M., and Tompkins, F. C., *Proc. Roy. Soc., Ser. A* **268,** 452 (1962).
18. Cukr, M., Merta, R., Adámek, J., and Ponec, V., *Collect. Czech. Chem. Commun.* **30,** 2682 (1965).
19. Horgan, A. M., and King, D. A., *in* "Adsorption-Desorption Phenomena" (F. Ricca, Ed.), p. 329. London, 1972.
20. Wedler, G., and Bröcker, F. J., *Surface Sci.* **26,** 454 (1971).
21. Wedler, G., Reichenberger, H., and Wenzel, H., *Z. Naturforsch.* **26a,** 1452 (1971).
22. Wedler, G., and Wissmann, P., *Surface Sci.* **26,** 389 (1971).
23. Suhrmann, R., Heyne, H. J., and Wedler, G., *J. Catal.* **1,** 208 (1962).
24. Wedler, G., and Fouad, M., *Z. Phys. Chem. (Frankfurt am Main)* **40,** 12 (1964).
25. Wedler, G., Papp, H., and Schroll, G., *Surface Sci.* **44,** 463 (1974).
26. Herrmann, A., dissertation, TH Hannover, 1960.
27. Bröcker, F. J., and Wedler, G., *Discuss. Faraday Soc.* **41,** 87 (1966).
28. Wedler, G., Bröcker, F. J., Fisch, G., and Schroll, G., *Z. Phys. Chem. (Frankfurt am Main)* **76,** 212 (1971).
29. Wedler, G., and Fisch, G., *Ber. Bunsenges. Phys. Chem.* **76,** 1160 (1972).
30. Wedler, G., and Schroll, G., *Z. Phys. Chem. (Frankfurt am Main)* **85,** 216 (1973).
31. Wedler, G., Fisch, G., and Papp, H., *Ber. Bunsenges. Phys. Chem.* **74,** 186 (1970).

32. Wedler, G., and Papp, H., *Z. Phys. Chem. (Frankfurt am Main)* **82,** 195 (1972).
33. Wedler, G., and Papp, H., unpublished data.
34. Wedler, G., and Strothenk, H., *Ber. Bunsenges. Phys. Chem.* **70,** 214 (1966).
35. Wedler, G., "Adsorption." Verlag Chemie, Weinheim/Bergstr., 1970.
36. Wedler, G., and Wissmann, P., *Z. Naturforsch.* **23a,** 1537, 1544 (1968).
37. Wedler, G., Wölfing, C., and Wissmann, P., *Surface Sci.* **24,** 302 (1971).
38. Pritchard, J., and Tompkins, F. C., *Trans. Faraday Soc.* **56,** 540 (1960).
39. Wedler, G., and Santelmann, G., *Ber. Bunsenges. Phys. Chem.* **75,** 1026 (1971).
40. Crossland, W. A., and Pritchard, J., *Surface Sci.* **2,** 217 (1964).
41. Suhrmann, R., Mizushima, Y., Herrmann, A., and Wedler, G., *Z. Phys. Chem. (Frankfurt am Main)* **20,** 332 (1959).
42. Wedler, G., and Borgmann, D., *Z. Phys. Chem. (Frankfurt am Main)* **74,** 64 (1971).
43. Papp, H., dissertation, Erlangen, 1972.
44. Wissmann, P., *Z. Phys. Chem. (Frankfurt am Main)* **71,** 294 (1970).